Cryogenic etching of silicon compounds using a CHF 3 based plasma

Rémi Dussart, R. Ettouri, J. Nos, G. Antoun, T. Tillocher, P. Lefaucheux

Journal of Applied Physics

AIP Publishing

Cryogenic etching of silicon compounds using a CHF_3 based plasma

R. Dussart[1*], R. Ettouri[1], J. Nos[1], G. Antoun[1], T. Tillocher[1], P. Lefaucheux[1],
[1]GREMI, Orléans University-CNRS, 14 Rue d'Issoudun BP 6744, 45067 Orléans, France
* remi.dussart@univ-orleans.fr

ABSTRACT

Cryogenic etching of a-Si, SiO_2 and Si_3N_4 materials by CHF_3/Ar inductively coupled plasma (ICP) are investigated in a range of temperature from -140°C to +20°C. Samples of the three different materials are placed together on a same silicon carrier wafer. Depending on the experimental conditions, etching or deposition regimes were obtained on the samples. The thickness variation was measured by spectroscopic ellipsometry. A process window between -120°C and -80°C was found in which Si_3N_4 surface is etched while CF_x deposition is obtained on a-Si and SiO_2 surfaces, resulting in an infinite etching selectivity of Si_3N_4 to the other materials. At high enough self-bias (-120V) and very low temperature (< -130°C), Si_3N_4 etch is reduced down to a very low value while a-Si and SiO_2 are still being etched, which inverses the selectivity between Si_3N_4 and the two other materials. EDX analyses of a Si_3N_4/a-Si/SiO_2 layer stack after a same etching process carried out at 20°C and -100°C confirm the presence of carbon and fluorine on a-Si at low temperature, showing the effect of the low temperature to switch from etching to deposition regime on this material.

Journal of Applied Physics

AIP Publishing

I. INTRODUCTION

Silicon compounds such as SiO_2 and Si_3N_4 are regularly used in microelectronics. They usually have to be structured with a high accuracy. In particular, in 3D NAND technology, Si_3N_4 and SiO_2 layers have to be etched alternatively until reaching the underlying silicon material without damaging it[1]. To form the 3D NAND devices, the stack of alternated layers must be etched without selectivity to form the channels[2]. Then, Si_3N_4, which is used as a sacrificial layer, has to be etched isotropically with a very high selectivity with SiO_2. Usually, hot phosphoric acid (H_3PO_4) is employed to wet etch Si_3N_4 between the SiO_2 layers [2].

Another key challenge in microelectronics relies on the Si_3N_4 spacer etch in CMOS technology, which must be very anisotropic, but performed with a high selectivity with the underlying Si or SiGe layer[3]. To achieve these demanding requirements and avoid the appearance of silicon recess, some special and complex plasma processes are currently under development [3,4].

Even if CHF_3 based plasma processes have been used a lot to etch SiO_2 [5–8] and Si_3N_4 [9,10] materials, this plasma chemistry is usually not sufficient to hit the highly critical dimensions that are expected at the nanoscale. For bigger dimensions, CHF_3 plasma usually offers a quite good selectivity between SiO_2 or Si_3N_4 with silicon due to the formation of a thicker CF_x polymer at the silicon surface, which is not consumed. CHF_3 gas can be mixed with O_2 to enhance the etch rate of Si_3N_4 and increase the selectivity with SiO_2, but the selectivity between the two materials remains of the order of 2 at best [9]. Most of experiments on SiO_2 and Si_3N_4 etch have been carried out on wafers maintained at a temperature beyond 0°C (typically at room temperature). In this paper, we investigate a CHF_3/Ar plasma etching process of silicon (Si), silicon nitride (Si_3N_4) and thermal silicon oxide (SiO_2) materials cooled at cryogenic temperature.

Cryogenic etching process was introduced in 1988 to perform anisotropic etching of silicon [11]. Cryo-etching of only few materials has been investigated so far including silicon [11–15], cobalt [16], II-VI materials [17,18] and SiOCH porous low-k materials [19–23]. It has been extensively used to etch high aspect ratio silicon structures [24,25]. A passivation based mechanism was proposed by Bartha *et al.* [26] and confirmed by many other different studies [14,15,27–31]. Although the cryogenic system to cool down the wafer to a very low temperature of typically -100°C might appear as a strong drawback, there are actually several advantages working at cryogenic temperature: the residence time of physisorbed species is higher on very cold surfaces [32]; the passivation layer is partly removed during the wafer warm up [28]; there is nearly no process drift since most of deposition occurs on low temperature surfaces, but not on the reactor wall.[15]

The etching of Si based material substrates cooled at a very low temperature in CHF_3/Ar plasma has not been reported so far. The influence of substrate temperature on the etch rates of PECVD SiN thin films has already been studied in CF_4/H_2 plasma, but the investigation was performed at a temperature between -20°C and +50°C.[33] However, very interesting results were obtained between – 20°C and 0°C, which show a clear evolution of surface compounds and etch rate of the PECVD SiN films depending on the bonding structures (concentration of Si-H or N-H sites). But, no experiment was reported at a temperature below -20°C. In the experiments reported in this paper, we varied the temperature between -140°C and +20°C and evaluated the etch rate of Si, SiO_2 and Si_3N_4 to determine the etch selectivity between them and define process windows with high selectivity. Finally, a material stack composed of SiO_2, a-Si and Si_3N_4 was etched and monitored by in-situ ellipsometry at two different temperatures: -100°C and +20°C. The surface composition of the 2 samples was qualitatively analyzed by EDX, confirming the etching of Si_3N_4 and the deposition of a quite thick CF_x layer on a-Si at very low temperature.

II. EXPERIMENTAL METHOD

The experiments are carried out in two different ICP reactors. A detailed schematic of the two reactors is provided in figures 1.a and 1.b. The cryogenic substrate holder of both reactors is cooled with liquid nitrogen and the temperature is controlled and stabilized using a Proportional Integral Derivative (PID) system. The temperature mentioned in the experimental conditions correspond to the set point temperature of the chuck. The two reactors are excited at 13.56 MHz and contain an alumina tube as a dielectric between the antenna and the reactor. The first reactor (Alcatel A601E) is equipped with an antenna consisting of 2 half turns, between which the current is separated before merging again at the opposite side (figure 1.a). The antenna of the second one (Oxford Instrument Plasma Pro 100 Cobra) consists of 4 turns around the alumina tube (figure 1.b). Even if there is a gas ring in the diffusion chamber of the second reactor, Ar and CHF_3 gases were injected from the gas inlet at the top of the reactors in both cases to maintain similar experimental conditions as much as possible. A distance as high as 30 cm separates the source from the table in the first reactor, whereas the separation is only 20 cm long in the second reactor. The second reactor is equipped with an in-situ spectroscopic ellipsometer (UVISEL Horiba Jobin Yvon). When using the first reactor, the samples were characterized by ex-situ ellipsometry.

Three different types of samples were used for the etch experiment. The composition of the different samples is schemed in figure 1c. The first one consists of a 100 nm thick layer of thermal SiO_2 on (100) silicon. The second one is composed of a 250 nm thick Si_3N_4 deposited by LPCVD on (100) silicon. The third one contains a 150 nm thick p-Si layer deposited by PECVD on a 100 nm layer of thermal SiO_2 grown on a (100) silicon wafer. The samples were cut into 2x2 cm^2 from 300 mm diameter wafers.

For each experiment, a sample of each type of material was glued with a thermally conductive paste on 100 or 150 mm carrier wafers of silicon as shown in figure 1d.

Some experiments have also been performed on samples consisting of a stack of deposited layers: thermal SiO_2 (100 nm), a-Si (60 nm) and Si_3N_4 (85 nm) deposited by PECVD in the clean room of GREMI laboratory (figure 1e).

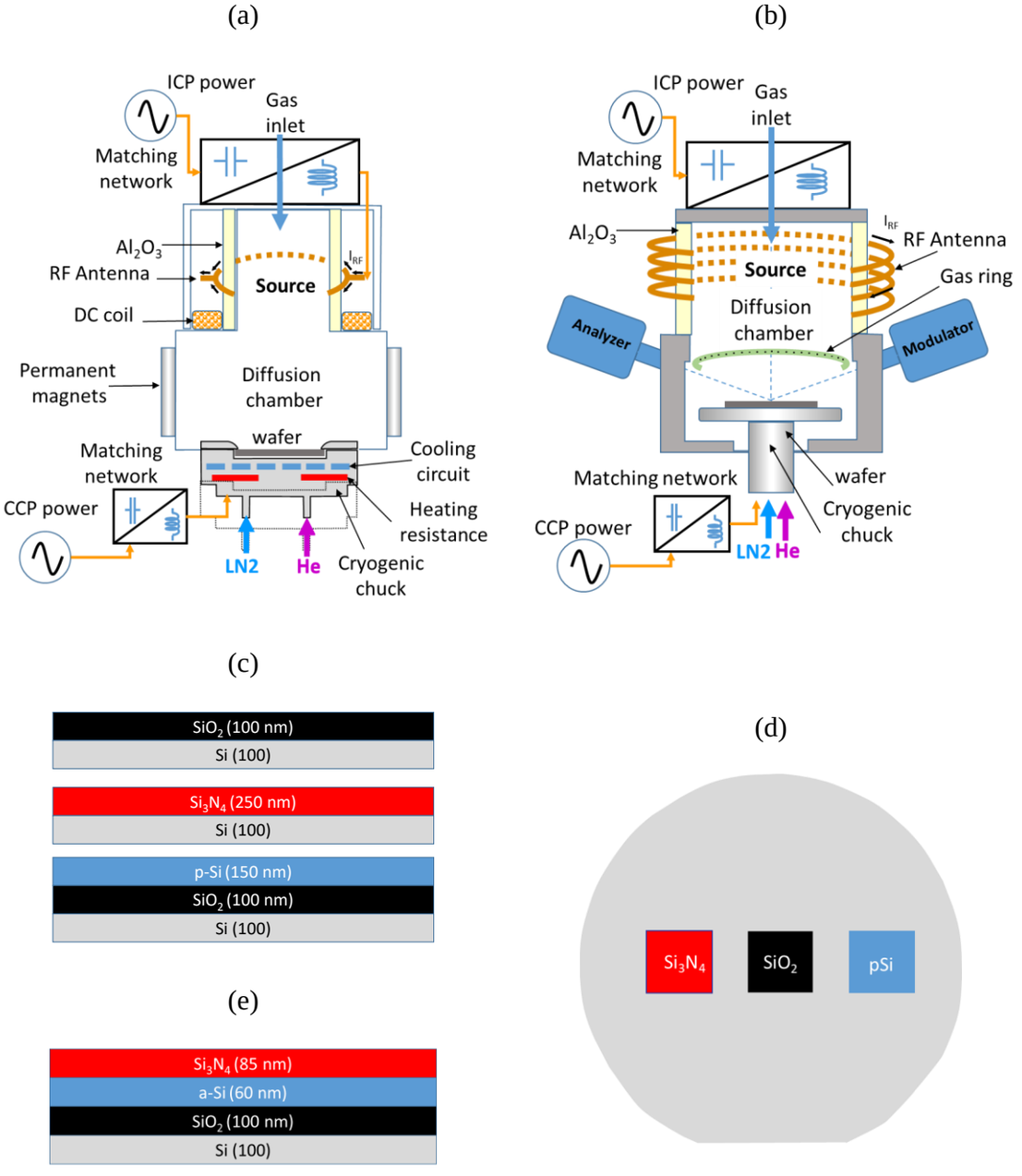

Figure 1: Experimental details

(a) Schematic of the reactor Alcatel A601E

(b) Schematic of the reactor Oxford Instrument Plasma Pro 100 Cobra

(c) Composition of the samples used for the etch experiments

(d) Sample arrangement on a 100 or 150 mm diameter silicon wafer

(e) Composition of the sample used for the layer stack etch experiment (prepared at GREMI laboratory)

The thickness of the deposited layer was accurately evaluated by ellipsometry before and after each experiment. A classical dispersion formula was used to model the SiO_2 layer whereas Si_3N_4, Si and CF_x layers were modeled using a new amorphous dispersion formula available on the DeltaPsi 2 software from Horiba/Jobin-Yvon. This software allows powerful numerical fittings of the measured delta psi ellipsometric angles in monochromator or in multi-wavelength kinetic mode monitoring the two angles at 32 selected photon energies between 1.5 and 5 eV. It was generally more difficult to model the CF_x layer. The fit parameter values varied with the chemical composition of the layer. However, some relevant ellipsometry model fittings were obtained with associated χ^2 values (goodness of fit) under than 5 which is appropriate.

After each etch process, the reactor was cleaned using a 10 min long oxygen plasma to avoid the accumulation of deposited CF_x layer on the reactor walls.

In the reference etching process, we used the parameters given in table 1.

CHF_3 flow	30 sccm
Ar flow	70 sccm
Pressure	1 Pa
Source Power	800 W
Bias voltage	80 V
Process duration	1 min
Set point temperature	-100°C

Table 1: Process parameters of the reference process

The elemental composition of the layers was performed on a Zeiss SUPRA-40 field emission Scanning Electron Microscope (SEM) using a Bruker Quantax EDS detector. Samples were mounted on SEM stubs secured by conductive clips, which eliminates contamination issues due to adhesives or glues.

III. RESULTS

The figure 2 shows the etched depth after 1 min of plasma process in the conditions provided in table 1 as a function of the bias voltage for 4 different temperatures between +20°C and -130°C. Negative values correspond to deposition regime.

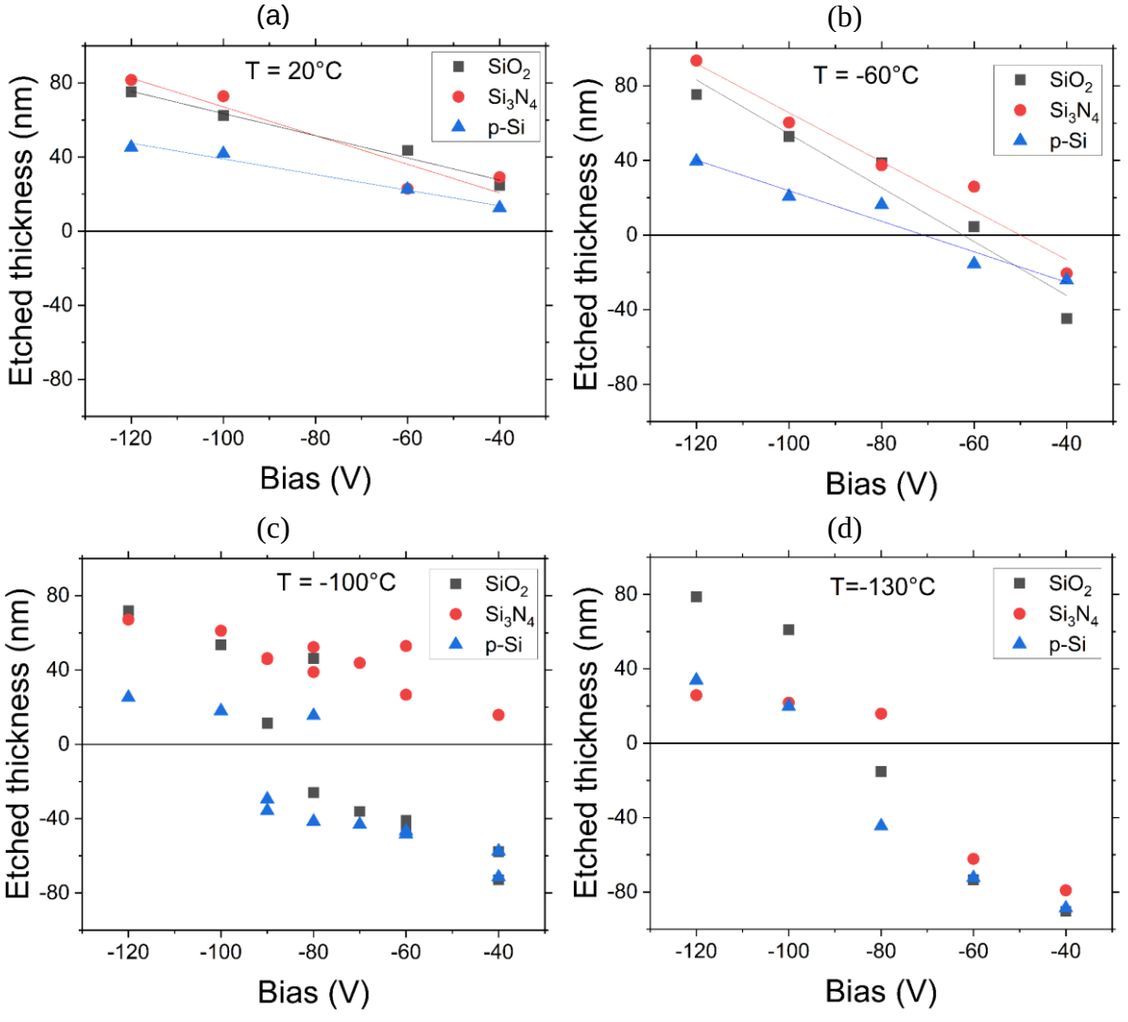

Figure 2 : Etched thickness of SiO_2, Si_3N_4 and p-Si versus bias at +20°C (a), -60°C (b), - 100°C (c) and -130°C (d) after 1 min of CHF_3/Ar plasma (30 sccm /70 sccm), P_{source} = 800 W, P = 1 Pa. Experiments performed on the first reactor (A601E).

At +20°C (figure 2.a), etching regime is obtained for all types of samples and for all values of bias voltage between -120V and -40V. The etch rate increases quite linearly with the applied

voltage as already reported in [8]. SiO_2 and Si_3N_4 etch rates are quite similar and reach a value between 20 and 25 nm/min at -40 V and 75 - 80 nm/min at -120V. The etch rate of p-Si is lower and reaches about 13 nm/min at -40 V and 45 nm/min at -120V. At this temperature, the etch selectivity between SiO_2 or Si_3N_4 and a-Si is lower than 2.

At -60°C (figure 2.b), about the same behavior as at +20°C is observed, but a depositing regime is reached for p-Si at -60 V bias voltage and for the 3 materials at -40 V. At -120V bias voltage, the etch rate is quite similar to the one obtained at +20°C.

When operating at -100°C (figure 2.c), depositing regime is attained between -80V and -40V for SiO_2 and p-Si whereas Si_3N_4 is still etched. We observe that the threshold between etching and deposition has moved to a bias voltage as high as -80V. At this very point, as can be seen from repetition of the experiment, etching or deposition was obtained for p-Si and SiO_2, which shows that the threshold between etching and deposition is quite sharp and that the process can easily switch from one regime to the other. It is also interesting to note that no deposition regime was observed on the Si_3N_4 sample at -100°C even at -40V bias voltage. The experiments have been performed twice at -100°C for -40 V and -60 V bias voltages (figure 2c) to check the reproducibility.

At -130°C (figure 2.d), the threshold between deposition and etching is obtained at around -80V, but in this case, we can notice that the etch rate of Si_3N_4 has significantly dropped from about 80 nm/min (at +20°C) to 25 nm/min, whereas p-Si and SiO_2 etch rates remain at the same value obtained at higher temperature. The selectivity between Si_3N_4 and the two other materials is inverted at -130°C at -120 V bias voltage. At -80V bias voltage, an etching regime for Si_3N_4 was reached whereas a deposition regime was occurring for SiO_2 and p-Si.

In figure 3, the etched or deposited thickness for the 3 materials is plotted versus temperature for 4 different bias voltages (-40V, -60V, - 100V and -120V) in the experimental conditions provided in table 1.

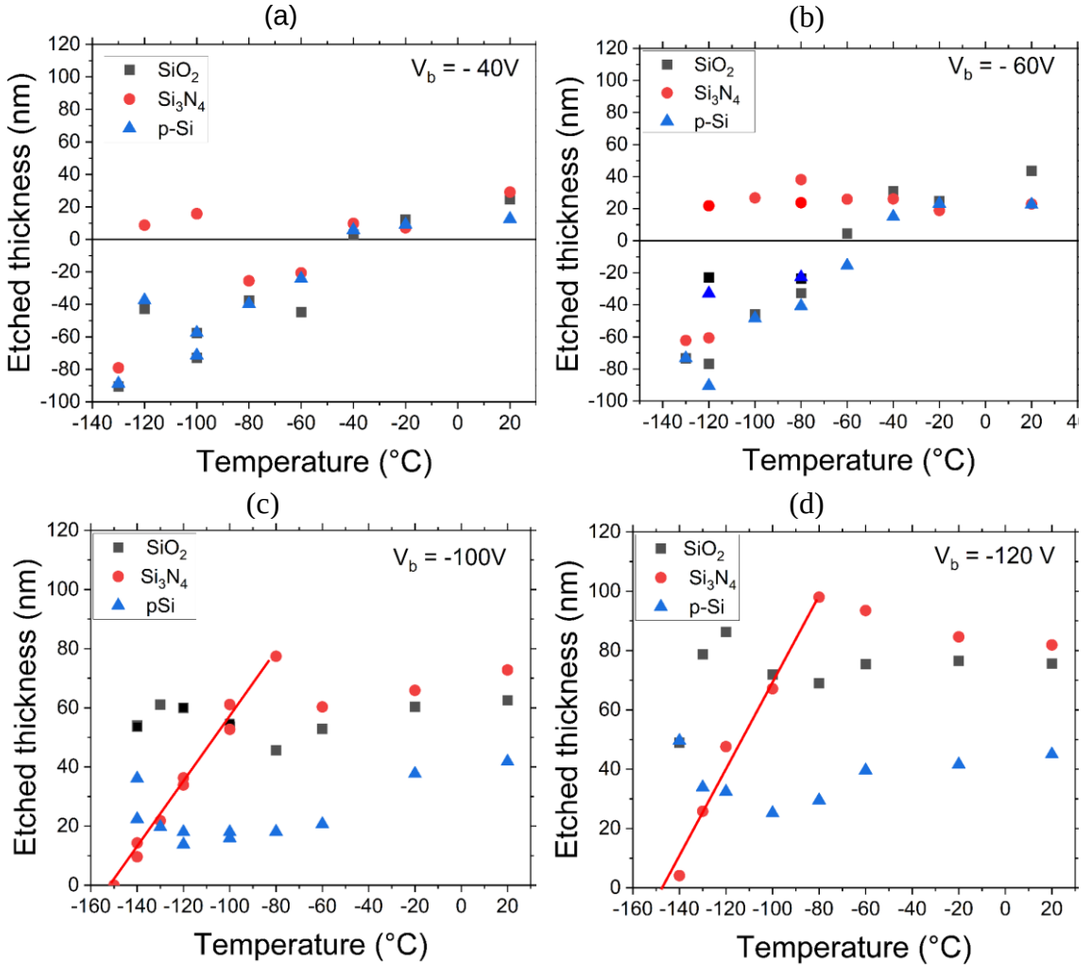

Figure 3 : Etched thickness of SiO_2, Si_3N_4 and p-Si versus temperature at -40 V (a), -60 V (b), -100 V (c) and -120 V (d) bias voltages after 1 min of CHF_3/Ar plasma (30 sccm /70 sccm), P_{source} = 800 W, P = 1 Pa. Experiments performed on the first reactor (A601E).

At -40 and -60V (figures 3a and 3b), we can clearly observe a threshold between etching and deposition for p-Si and SiO_2 by decreasing the temperature. At -40V bias voltage, deposition regime is obtained at a temperature between -40 and -60°C ; At -60V bias voltage, deposition

regime is reached at a temperature between -60 and -80°C. The higher the bias voltage, the lower the temperature to reach the threshold.

At -100 and -120V bias voltage (figures 3c and 3d), p-Si and SiO_2 materials are etched regardless of the temperature. Note that additional measurement points have been carried out at -100V at -100°C, -120°C and -140°C to check the reproducibility of the data. The etch rate tends to decrease when the temperature decreases down to -100°C for p-Si and down to -80°C for SiO_2. In the case of SiO_2, it increases again down to -120°C before dropping at -140°C. In the case of p-Si, the etch rate keeps increasing from -100°C to -140°C especially at -120V bias voltage.

For silicon nitride, at -40V, the etch rate is close to the one obtained with the two other materials, except at -100°C and -120°C, for which deposition occurs on SiO_2 and p-Si, but not on Si_3N_4. At -60V, silicon nitride is etched at the same rate regardless of the temperature. At this bias voltage (figure 3b), a window of infinite etch selectivity between -120°C and -60°C appears between silicon nitride and the two other materials. Below -120°C, a deposition regime was reached for Si_3N_4. At -100V bias voltage, the etch rate of silicon nitride is more or less constant down to -100°C, but decreases quite linearly between -100°C and -150°C. At -140°C, the selectivity is inversed between silicon nitride and the 2 other materials. This behavior is also observed at -120V bias voltage where Si_3N_4 etching drops linearly when the temperature is varied from -80°C to -140°C.

The figure 4 shows the estimated bias voltage threshold between deposition and etching regimes for the three different materials versus temperature, evaluated from the graphs shown in figure 2 and other experiments performed at -120°C, -80°C and -20°C. The error bars correspond to the bias increment, which was employed to plot the graph of figure 2 (10, 15 or 20V). By decreasing the temperature, one has to apply a higher bias voltage to switch from deposition to etch regime. The bias voltage threshold is lower (in absolute value) for Si_3N_4. At -100°C, the threshold gap

between Si_3N_4 and the two other materials widens in bias voltage. Indeed, at -40V on figure 3.a, we can notice that deposition regime is reached for Si_3N_4 at -60 and -80°C, but etching regime is obtained again at -100°C and -120°C.

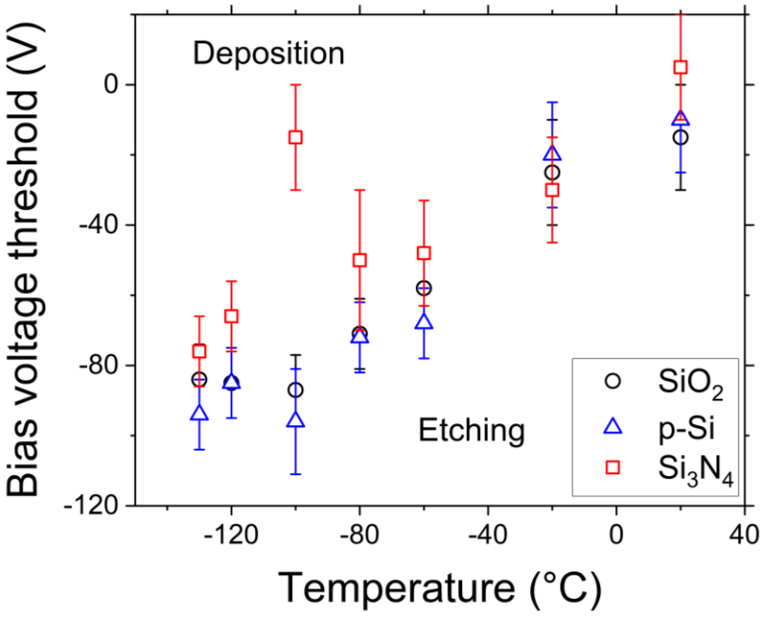

Figure 4: Bias voltage threshold between deposition and etching versus temperature.

Error bars are estimated from the bias increment that was used to plot the graph of figure 2.

In-situ experiments were carried out on the other reactor (Oxford Instruments Plasma Pro 100 Cobra) equipped with a spectroscopic ellipsometer. The thickness evolution of the 3 materials is shown in figure 5 at +20°C and -100°C.

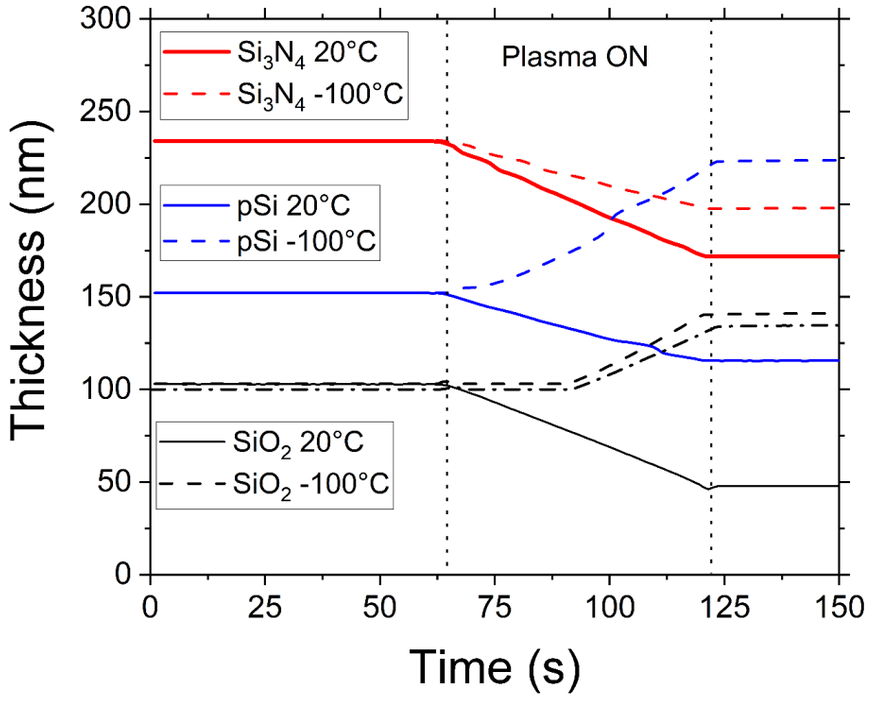

Figure 5: In-situ etching measurements of the etched thickness of p-Si, Si_3N_4 and SiO_2 at 20°C (solid-line) and at -100°C (dashed-line). Experiments performed on the second reactor (Oxford Instruments Plasma Pro100 Cobra).

The experimental conditions are those provided in table 1 with a bias voltage as high as -80 V. The plasma of CHF_3/Ar is initiated after 60s. At 20°C, etching is obtained for the 3 materials. The etch rate of Si_3N_4, p-Si and SiO_2 is 65 nm.min^{-1}, 38 nm.min^{-1} and 59 nm.min^{-1} respectively at +20°C. At -100°C, the etching regime is maintained for silicon nitride only. The etch rate of Si_3N_4 is lower at -100°C: it reaches 38 nm.min^{-1} at -100°C instead of 65 nm.min^{-1} at +20°C. Deposition is obtained for both SiO_2 and p-Si at -100°C. Interestingly, the deposition on SiO_2 does not start immediately after the CHF_3/Ar plasma ignition: it takes about 30s before the deposition starts. The experiment was repeated to confirm this result and is reproducible as it can be observed on figure 5 (dash dot dash line). This delay for deposition is not observed on p-Si, for which the growth starts immediately when the plasma is on.

In order to confirm the results presented in previous parts, two etch experiments were carried out on a layer stack composed of 85 nm of Si_3N_4, 60 nm of a-Si and 100 nm of SiO_2 deposited by PECVD (as schemed in figure 1c). The experiments were performed in the second ICP tool (Oxford Instruments Plasma Pro 100 Cobra) at +20°C and at -100°C in the experimental conditions provided in table 1, except for the bias voltage which was a little bit higher due to a technical issue on the etcher: -90V instead of -80V. The thickness time evolution was monitored by in-situ ellipsometry. The results at +20°C are shown in figure 6.a. We can observe the thickness variation of the three materials, successively etched with a different etch rate, starting with Si_3N_4. The evaluated etch rate was 93 $nm.min^{-1}$ for Si_3N_4, 44 $nm.min^{-1}$ for a-Si and 55 $nm.min^{-1}$ for SiO_2. The etch rate is a little higher than the one shown in figure 5. It can be explained by the fact that the deposited Si_3N_4 is probably different from the one prepared by Tokyo Electron. Moreover, the bias voltage was slightly higher in this experiment. At -100°C (figure 6.b), in the same experimental conditions, we can observe the etching of Si_3N_4 with an etch rate of 39 $nm.min^{-1}$, which, this time, is quite closed to the one estimated from figure 5 in the previous experiment. Then, when the Si_3N_4 is completely etched, CF_x deposition starts on a-Si at a deposition rate of 75 $nm.min^{-1}$. Note that it was difficult to model the deposition on a-Si immediately after the etching in kinetic mode since the kinetic ellipsometry model does not simultaneously allow the simulation of a material that is etched followed by the deposition of another material. This is the reason why we did not plot the thickness time evolution between 174 and 196 seconds on figure 6b. But, we could individually model some of the delta-psi graphs obtained at different times during the deposition regime (open circles in figure 6.b). The results give an estimated thickness value very consistent with the one obtained by the kinetic model (solid line).

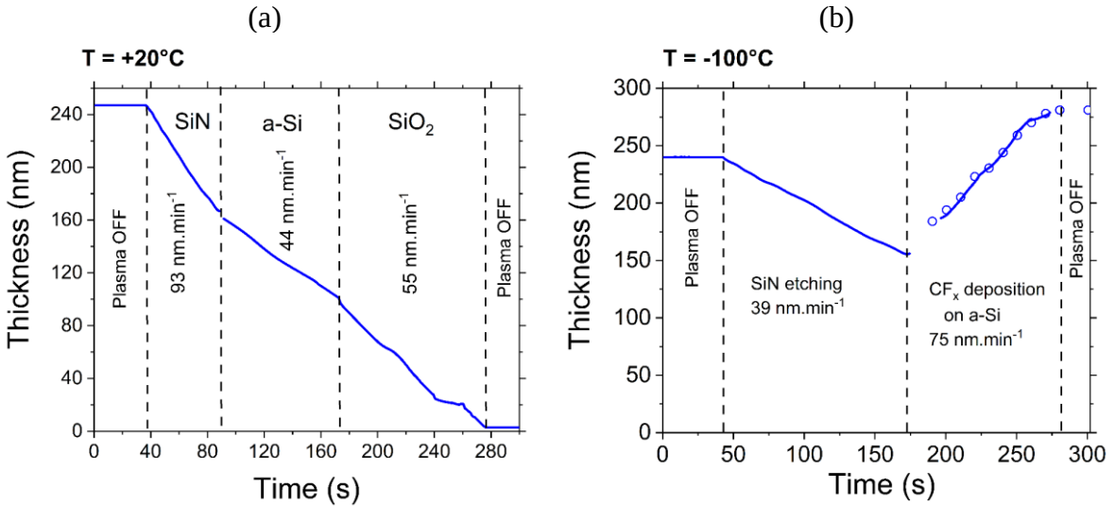

Figure 6: Thickness time evolution of the stack composed of SiO_2, a-Si and Si_3N_4 with a plasma of CHF_3/Ar in the experimental conditions given in table 1 at +20°C (a). Thickness time evolution of the same stack and experimental conditions, but at -100°C. Experiments performed on the second reactor (Oxford Instruments Plasma Pro100 Cobra) (b).

Then, the samples were analyzed by EDX before and after the etch experiments. The chemical analysis of a pristine sample is shown in figure 7 ('reference' spectrum) together with the chemical analysis of the samples treated at +20°C and at -100°C. The concentration of the major elements in atomic percentage is given in table 2.

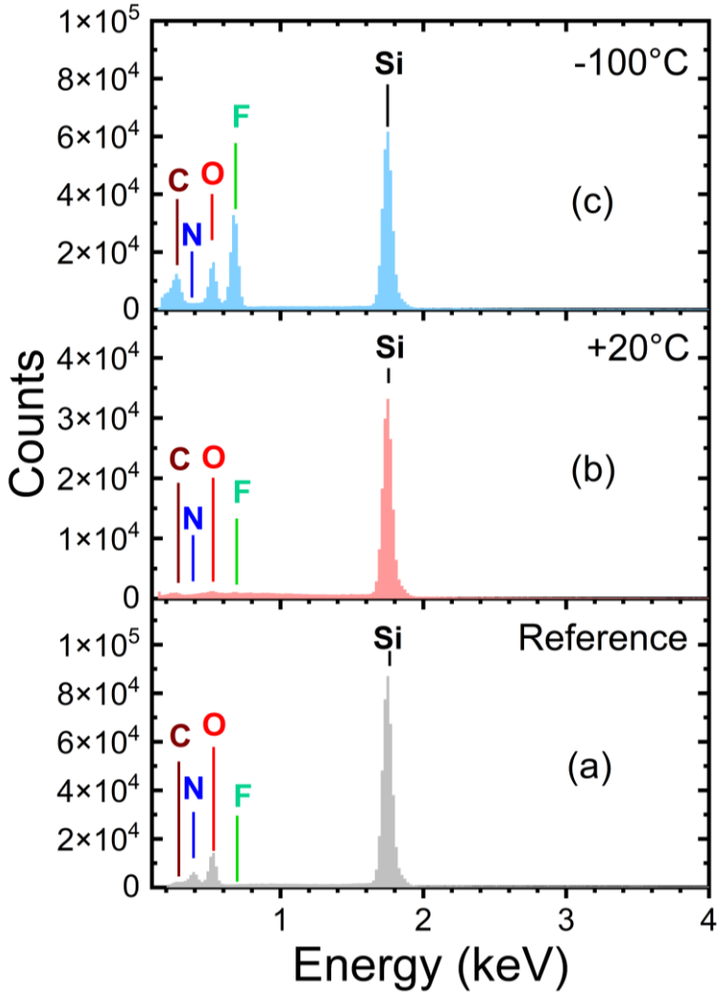

Figure 7: Energy-dispersive X-ray spectrum (EDS) of the reference sample (pristine) (a), the sample etched at +20°C (b) and the sample etched at -100°C (c)

Element	C(%)	N(%)	O(%)	F(%)	Si(%)
Pristine	10.8	18.9	20.0	0.5	49.8
+20°C	10.1	4.0	2.1	0.9	82.9
-100°C	31.0	5.3	14.9	23.0	25.8

Table 2: Concentration of major elements in atomic percentage (At.%) on a pristine sample and on the samples treated by a CHF_3/Ar plasma at +20°C and -100°C

In the pristine sample, we can observe peaks attributed to silicon, oxygen and nitrogen coming from the different layers present at the surface. We also have a little bit of carbon due to contamination, but the fluorine line is hardly observable and its estimated atomic percentage is 0.5 %. At +20°C, we mainly detect silicon. The atomic percentage of the other elements is below 5 % except for carbon (10.1 %), again due to contamination or due to remaining carbon coming from the CHF_3/Ar plasma. After the etch experiment at -100°C, we obtained a high percentage of carbon (31.0 %) and fluorine (23.0 %) which correspond to the CF_x deposited layer. The percentage of nitrogen is below 5%, which indicates that the Si_3N_4 layer has been etched completely. The oxygen percentage is 14.9%, which probably corresponds to the SiO_2 layer under the a-Si layer.

IV. DISCUSSION

By decreasing the substrate temperature from +20°C down to – 130°C, very different behaviors can be obtained on silicon based materials interacting with CHF_3/Ar plasma. At room temperature, the three types of sample are etched whatever the bias voltage is between -120V and -40V. At low temperature and a bias voltage of -60V, a deposition regime is obtained on SiO_2 and Si, but not on Si_3N_4 leading to an infinite etch selectivity. In a previous paper[34], we have reported quasi in-situ experiments and showed that the concentration of the different species present at the surface after a SiF_4/O_2 plasma could be significantly modified by decreasing the temperature to very low values (typically -100°C). In particular, the fluorine concentration was much higher at -100°C than at -65°C or -40°C. This effect was attributed to SiF_x physisorption, which seems to be more efficient at very low temperature, favoring reactions with oxygen at the surface to form the SiO_xF_y layer. Using CHF_3/Ar plasma instead of SiF_4/O_2 plasma, we can assume that CF_x species have a longer residence time at the surface at low temperature, favoring polymerization mechanisms. This can explain the enhanced deposition under low temperature and low self-bias voltage conditions for all materials.

However, this deposition regime is not systematically observed in the case of Si_3N_4 at low temperature, for which etch regime is still observed, but at a lower rate. In the case of Si_3N_4, the consumption of fluorine seems to be more pronounced, probably due to the formation of NF_3. But, a deposition regime should be reached for a higher flow of CF_x at the surface.

A higher etch selectivity between Si_3N_4 and a-Si at low temperature in a SiF_4/O_2 plasma has already been reported [35]. But, this higher selectivity was obtained at a temperature of -65°C whereas it collapsed at -100°C. The results were interpreted after in-situ XPS analysis, which showed that the fluorine concentration at the surface was quite different on the two surfaces of a-Si and Si_3N_4 at -65°C. In the case of CHF_3, we can assume that the surface chemical composition should also vary versus temperature, as it has been shown as well by Hsiao *et al.*[33] in CF_4/H_2 plasma.

As shown in figure 4, it is possible to avoid deposition on p-Si or on SiO_2, and switch to etch regime by increasing the bias voltage. The threshold voltage between the two regimes increases as the temperature decreases. However, at high enough bias voltage ($|V_{bias}| > 100V$) we could observe a collapse of the Si_3N_4 etch rate when decreasing the temperature from -100°C to -130°C whereas etch rate of p-Si tends to increase. It should be noted that the Si_3N_4 etch rate decreases quite linearly with temperature (see figures 3c and 3d). This point is not yet quite well understood, but it could be due to the presence of water at the surface, which starts to physisorb more significantly in this range of temperature at the working pressure of the experiment [36], and could modify the chemical kinetic at the surface. In particular, the concentration of the different bonding structures in Si_3N_4 (Si–H or N–H) can play an role H important role as mentioned in [33], exhibiting an opposite tendency as a function of substrate temperature. It is worth noting that the etching selectivity between Si_3N_4 and p-Si can be inversed at -140°C at high bias voltage ($|V_{bias}| > 100V$) whereas all other experimental conditions are kept the same.

V. CONCLUSION

Cryogenic etching was performed using CHF_3/Ar plasma on 3 different types of silicon based materials: SiO_2, Si_3N_4 and p-Si or a-Si. By decreasing the temperature down to a value between -60°C and -120°C, an infinite etch selectivity can be obtained between Si_3N_4 and Si or SiO_2 at a bias voltage of the order of -60V. At very low temperature (-140°C) and a high bias voltage (-120V), the selectivity can be inversed. At -120V bias voltage, the Si_3N_4 etch rate first increases by decreasing the temperature, and suddenly drops by lowering the temperature until reaching a very low etch rate. The threshold between etch and deposition regions was plotted versus bias voltage and temperature for the three types of material. At -100°C, the threshold gap between Si_3N_4 and the two other materials is wider in bias voltage, which offers a quite interesting process window to maintain the etch selectivity. At this temperature of -100°C, in-situ ellipsometric measurements were carried out showing that deposition starts immediately when the plasma is initiated on Si at low temperature, but with a delay of few seconds on SiO_2 at low temperature. In-situ measurements were also performed on a layer stack composed of SiO_2, a-Si and Si_3N_4 at +20°C and -100°C. At low temperature, deposition occurs on a-Si as soon as the whole Si_3N_4 layer is etched whereas the three different layers are etched at room temperature. EDS analysis gave very consistent results showing the presence of fluorine and carbon on the sample treated at low temperature, whereas silicon was mainly detected on the sample treated at room temperature. The temperature of the sample offers another set of very interesting and promising process opportunities in the cryogenic range to modify the chemistry at the surface. The residence time of radicals provided by the plasma can be longer and favor some chemical reactions. In the case of CHF_3, polymerization is favored at low temperature on silicon and SiO_2. On Si_3N_4, this mechanism does not occur at the same temperature, showing that the chemistry at the surface is quite different.

ACKNOWLEDGEMENT

The authors gratefully thank Tokyo Electron Limited for providing the wafers and for their support. This work was supported by CERTeM 5.0 platform, which provides most of the equipment. It is also supported by ANR, under the project name PSICRYO (No. ANR-20-CE24-0014).

AUTHOR DECLARATIONS

CONFLICT OF INTEREST

The authors have no conflicts of interest to declare.

DATA AVAILABILITY

The data that support the findings of this study are available from the corresponding author upon reasonable request

REFERENCES

[1] T. Reiter, X. Klemenschits, and L. Filipovic, Solid-State Electronics **192**, 108261 (2022).

[2] C.G.N. Lee, K.J. Kanarik, and R.A. Gottscho, J. Phys. D: Appl. Phys. **47**, 273001 (2014).

[3] V. Renaud, C. Petit-Etienne, J.-P. Barnes, J. Bisserier, O. Joubert, and E. Pargon, Journal of Applied Physics **126**, 243301 (2019).

[4] R. Blanc, F. Leverd, T. David, and O. Joubert, J. Vacuum Sci. Technol. B, **31**, 051801 (2013).

[5] G.Y. Yeom and M.J. Kushner, Appl. Phys. Lett. **56**, 857 (1990).

[6] S. Samukawa and S. Furuoya, Jpn. J. Appl. Phys. **32**, L1289 (1993).

[7] T. Fukasawa, A. Nakamura, H. Shindo, and Y. Horiike, Jpn. J. Appl. Phys. **33**, 2139 (1994).

[8] F. Gaboriau, G. Cartry, M.-C. Peignon, and Ch. Cardinaud, J. Vac. Sci. Technol. B **20**, 1514 (2002).

[9] L. Chen, L. Xu, D. Li, and B. Lin, Microelectronic Engineering **86**, 2354 (2009).

[10] T.E.F.M. Standaert, C. Hedlund, E.A. Joseph, G.S. Oehrlein, and T.J. Dalton, J. Vac. Sci. Technol. A **22**, 53 (2004).

[11] S. Tachi, K. Tsujimoto, and S. Okudaira, Appl. Phys. Lett. **52**, 616 (1988).

[12] H. Jansen, M. de Boer, and M. Elwenspoek, in *Proceedings of Ninth International Workshop on Micro Electromechanical Systems* (IEEE, San Diego, CA, USA, 1996), pp. 250–257.

[13] M. Boufnichel, S. Aachboun, F. Grangeon, P. Lefaucheux, and P. Ranson, J. Vac. Sci. Technol. B **20**, 1508 (2002).

[14] T. Tillocher, R. Dussart, X. Mellhaoui, P. Lefaucheux, N.M. Maaza, P. Ranson, M. Boufnichel, and L.J. Overzet, J. Vac. Sci. Technol. A **24**, 1073 (2006).

[15] R. Dussart, T. Tillocher, P. Lefaucheux, and M. Boufnichel, J. Phys. D: Appl. Phys. **47**, 123001 (2014).

[16] D. Staaks, X. Yang, K.Y. Lee, S.D. Dhuey, S. Sassolini, I.W. Rangelow, and D.L. Olynick, Nanotechnology **27**, 415302 (2016).

[17] Y.Y. Chen, Z.H. Ye, C.H. Sun, S. Zhang, X.N. Hu, R.J. Ding, and L. He, Infrared Technology and Applications XLII conference, Proc. of SPIE p. 981922.

[18] F.L. Liu, Y.Y. Chen, Z.H. Ye, R.J. Ding, and L. He, infrared Technology and Applications XLIII, Proc. of SPIE Vol. 10177.

[19] L. Zhang, R. Ljazouli, P. Lefaucheux, T. Tillocher, R. Dussart, Y.A. Mankelevich, J.-F. de Marneffe, S. de Gendt, and M.R. Baklanov, ECS Solid State Letters **2**, N5 (2012).

[20] L. Zhang, R. Ljazouli, P. Lefaucheux, T. Tillocher, R. Dussart, Y.A. Mankelevich, J.-F. de Marneffe, S. de Gendt, and M.R. Baklanov, ECS J. Solid State Sci. Technol. **2**, N131 (2013).

[21] F. Leroy, L. Zhang, T. Tillocher, K. Yatsuda, K. Maekawa, E. Nishimura, P. Lefaucheux, J.-F. de Marneffe, M.R. Baklanov, and R. Dussart, J. Phys. D: Appl. Phys. **48**, 435202 (2015).

[22] A. Rezvanov, A.V. Miakonkikh, A.S. Vishnevskiy, K.V. Rudenko, and M.R. Baklanov, J. Vac. Sci. Technol. B, **35**, 021204 (2017).

[23] R. Chanson, L. Zhang, S. Naumov, Yu.A. Mankelevich, T. Tillocher, P. Lefaucheux, R. Dussart, S.D. Gendt, and J.-F. de Marneffe, Sci Rep **8**, 1886 (2018).

[24] H. Jansen, M. de Boer, H. Wensink, B. Kloeck, and M. Elwenspoek, Microelectronics Journal **32**, 769 (2001).

[25] S. Aachboun, P. Ranson, C. Hilbert, and M. Boufnichel, J. Vac. Sci. Technol. A **18**, 1848 (2000).

[26] J.W. Bartha, J. Greschner, M. Puech, and P. Maquin, Microelectronic Engineering **27**, 453 (1995).

[27] M.J. de Boer, J.G.E. Gardeniers, H.V. Jansen, E. Smulders, M.-J. Gilde, G. Roelofs, J.N. Sasserath, and M. Elwenspoek, J. Microelectromech. Syst. **11**, 385 (2002).

[28] R. Dussart, M. Boufnichel, G. Marcos, P. Lefaucheux, A. Basillais, R. Benoit, T. Tillocher, X. Mellhaoui, H. Estrade-Szwarckopf, and P. Ranson, J. Micromech. Microeng. **14**, 190 (2004).

[29] X. Mellhaoui, R. Dussart, T. Tillocher, P. Lefaucheux, P. Ranson, M. Boufnichel, and L.J. Overzet, Journal of Applied Physics **98**, 104901 (2005).

[30] R. Dussart, X. Mellhaoui, T. Tillocher, P. Lefaucheux, M. Boufnichel, and P. Ranson, Microelectronic Engineering **84**, 1128 (2007).

[31] J. Pereira, L.E. Pichon, R. Dussart, C. Cardinaud, C.Y. Duluard, E.H. Oubensaid, P. Lefaucheux, M. Boufnichel, and P. Ranson, Appl. Phys. Lett. **94**, 071501 (2009).

[32] S. Tinck, E.C. Neyts, and A. Bogaerts, J. Phys. Chem. C **118**, 30315 (2014).

[33] S.-N. Hsiao, K. Nakane, T. Tsutsumi, K. Ishikawa, M. Sekine, and M. Hori, Applied Surface Science **542**, 148550 (2021).

[34] G. Antoun, A. Girard, T. Tillocher, P. Lefaucheux, J. Faguet, K. Maekawa, C. Cardinaud, and R. Dussart, ECS J. Solid State Sci. Technol. **11**, 013013 (2022).

[35] G. Antoun, T. Tillocher, A. Girard, P. Lefaucheux, J. Faguet, H. Kim, D. Zhang, M. Wang, K. Maekawa, C. Cardinaud, and R. Dussart, J. Vac. Sci. & Technol. A **40**, 052601 (2022).

[36] G. Antoun, T. Tillocher, P. Lefaucheux, J. Faguet, K. Maekawa, and R. Dussart, Sci Rep **11**, 357 (2021).

(a)

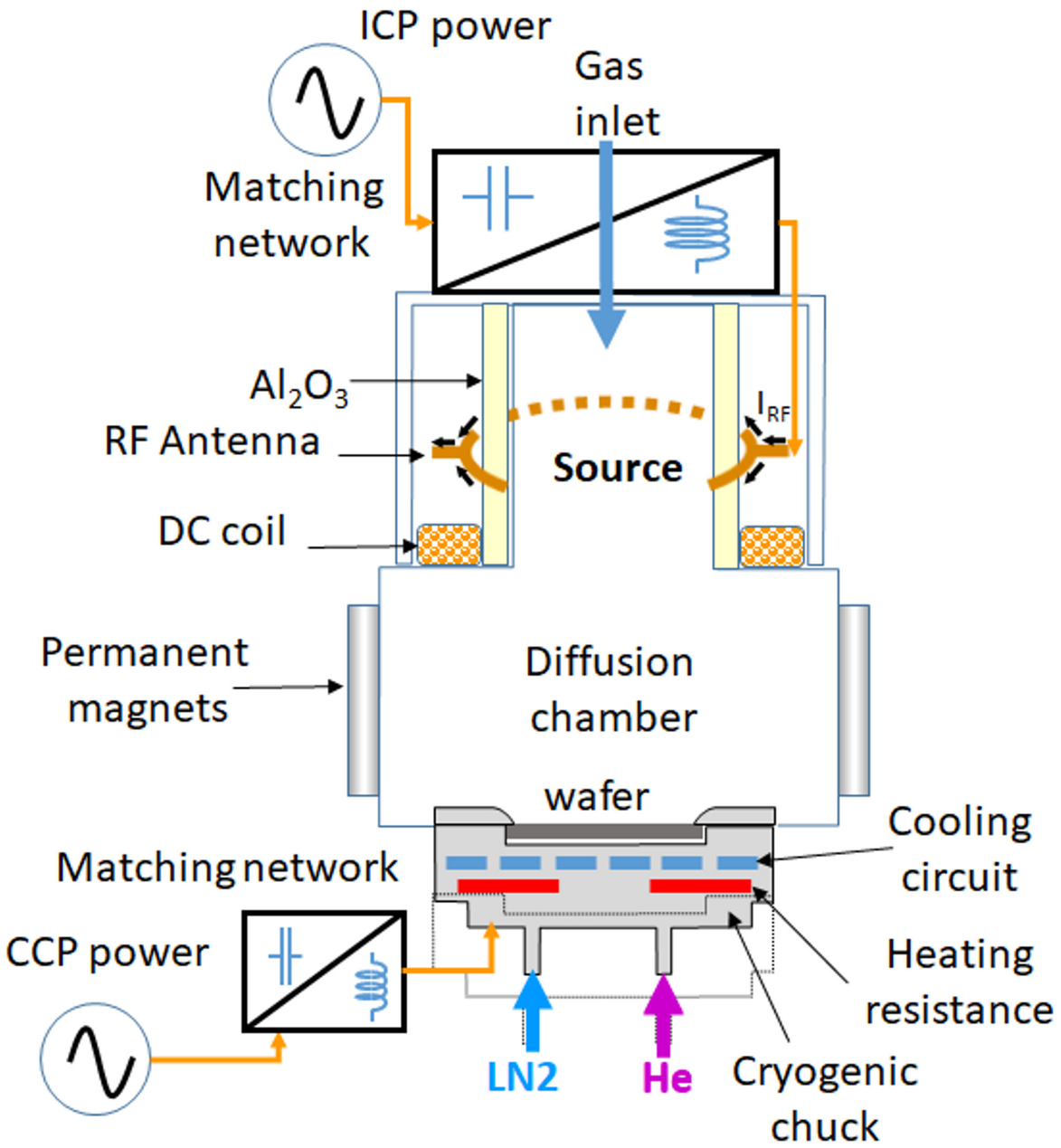

(c)

(d)

(b)

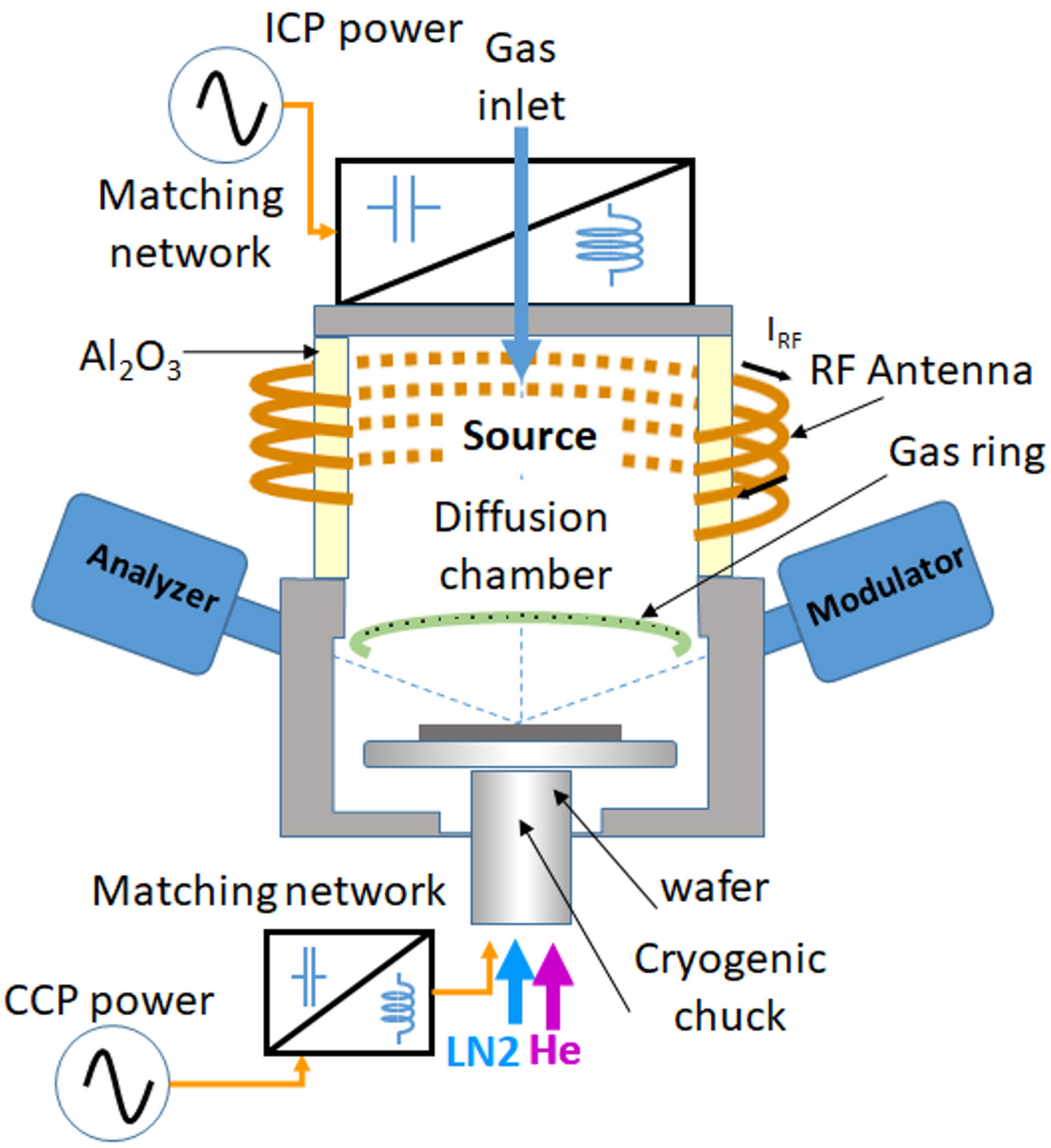

(e)

(a)

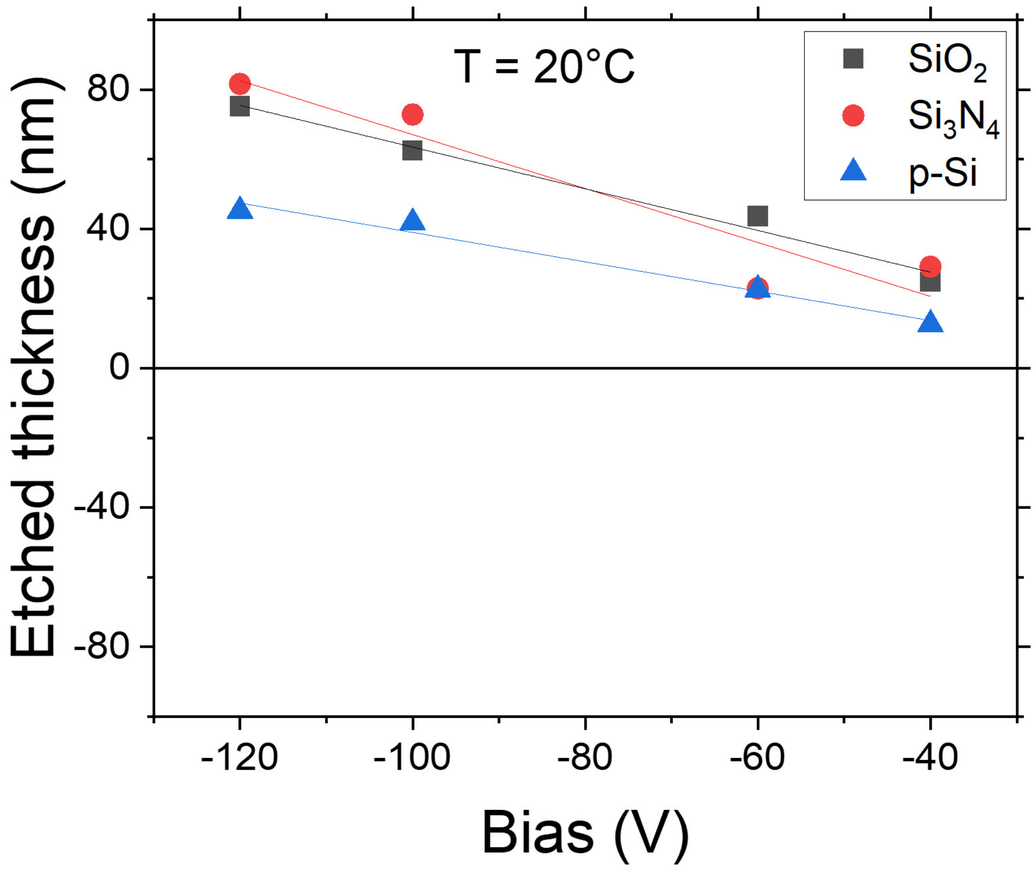

(b)

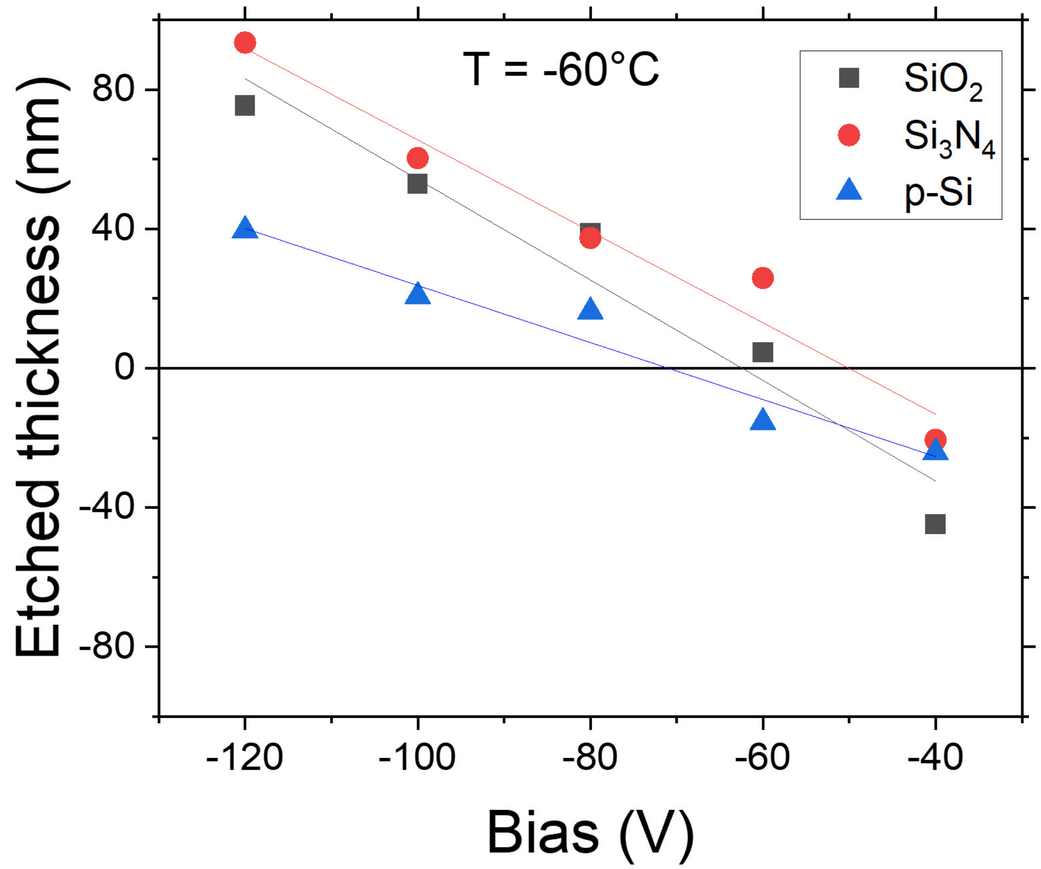

(c)

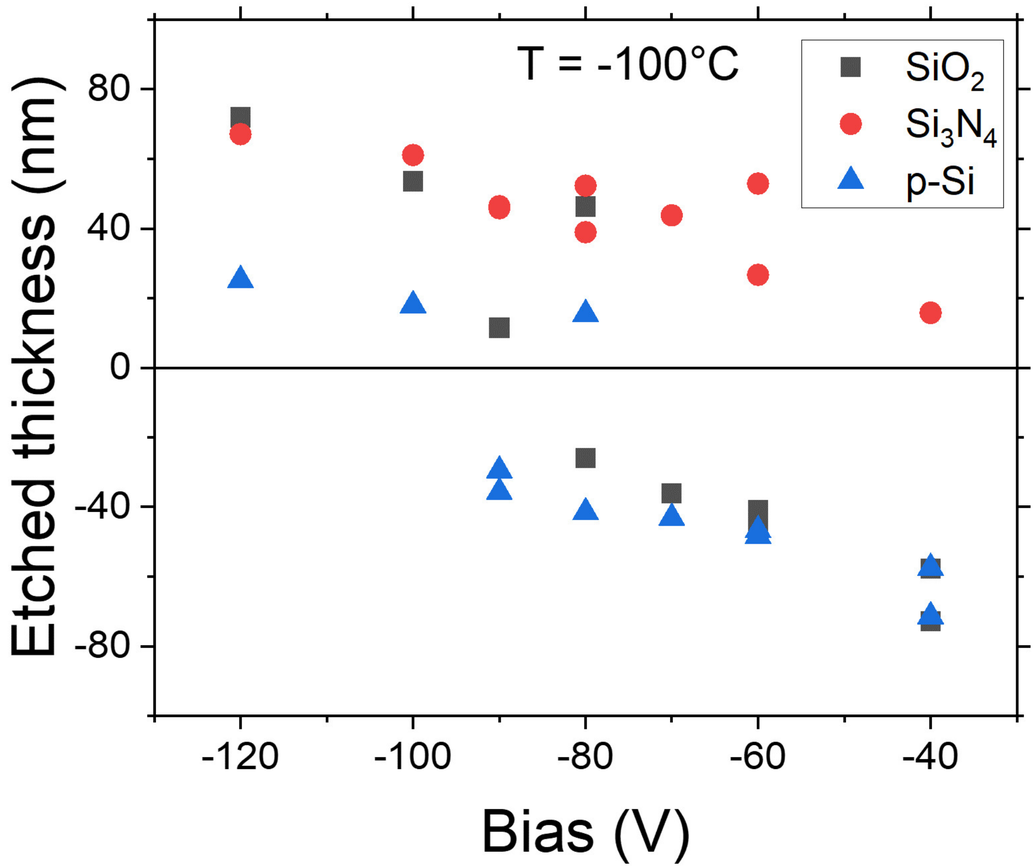

(d)

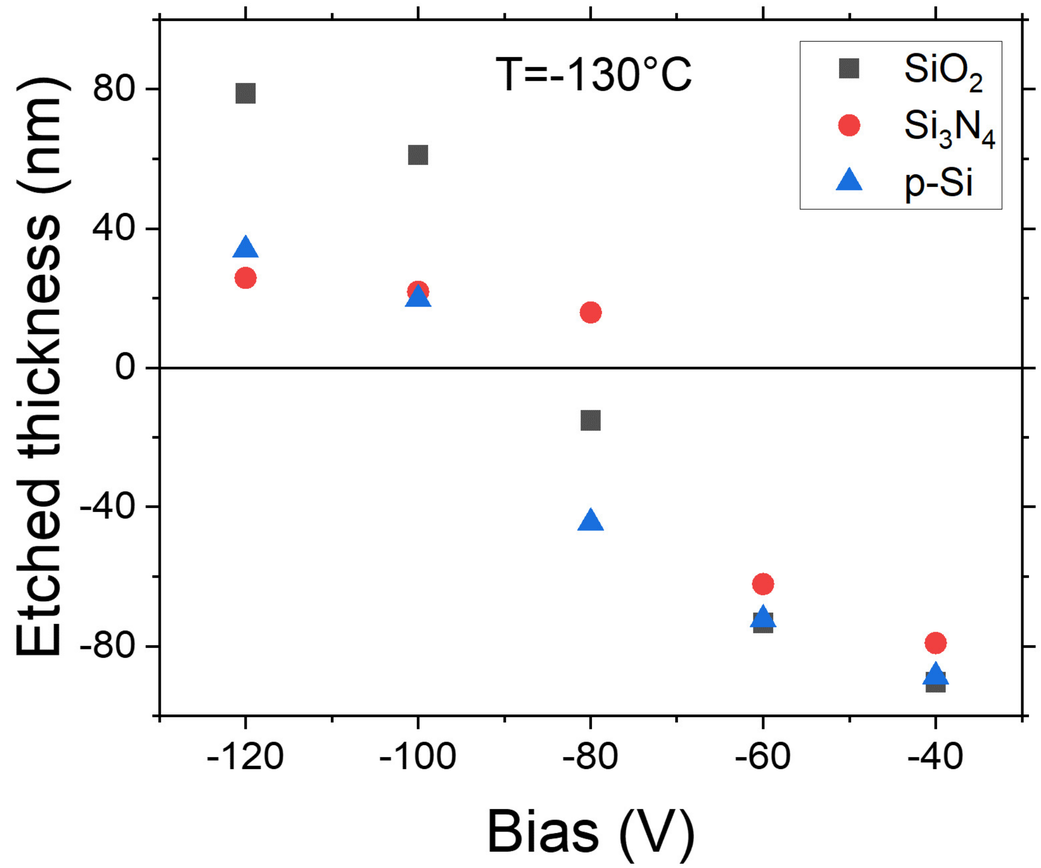

(a)

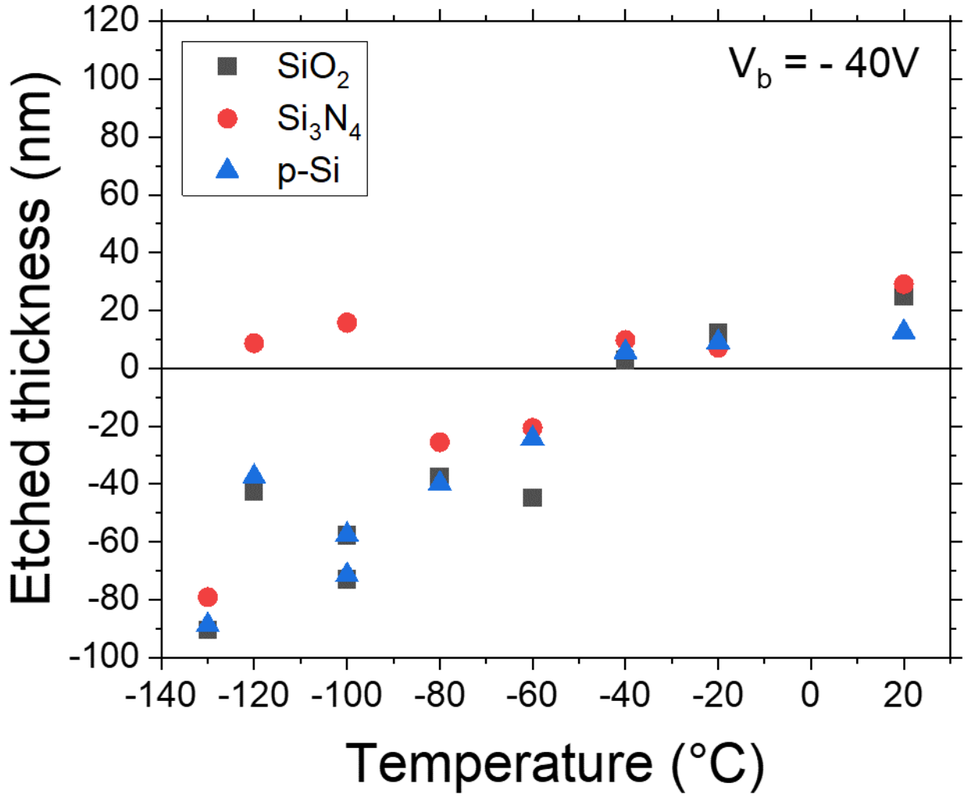

(b)

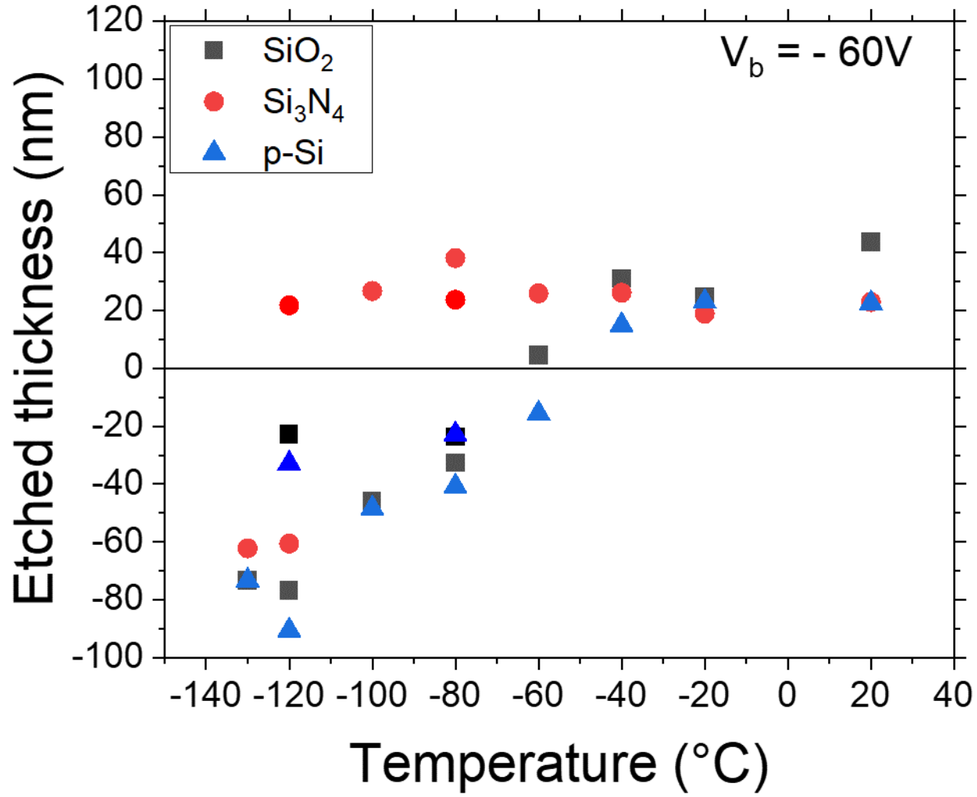

(c)

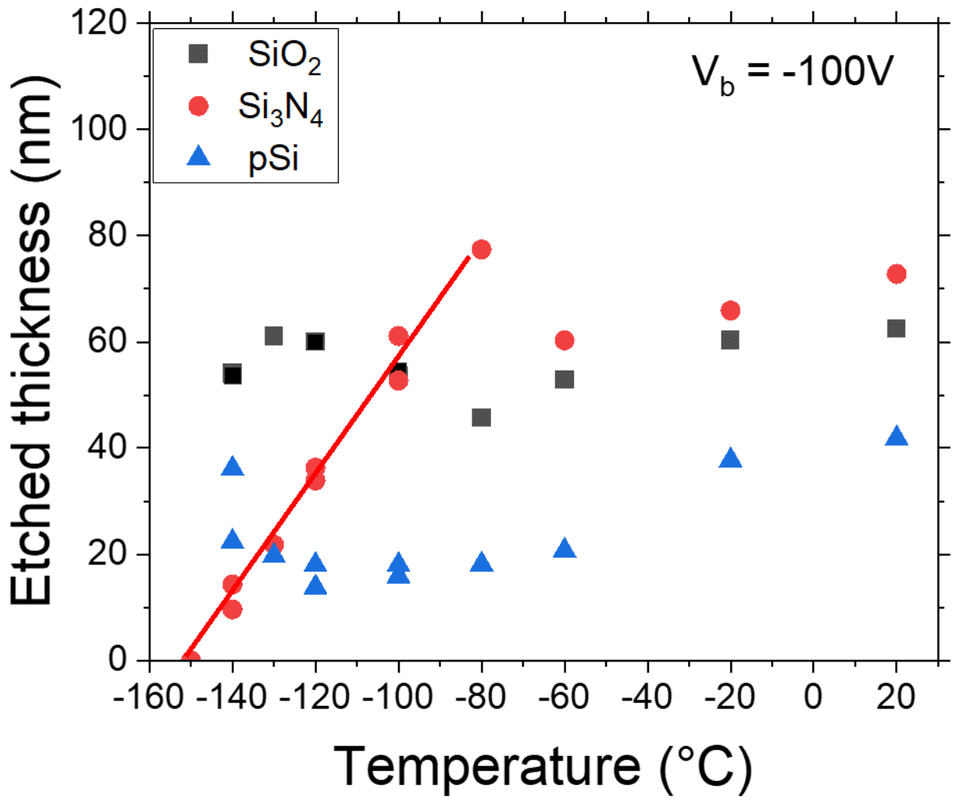

(d)

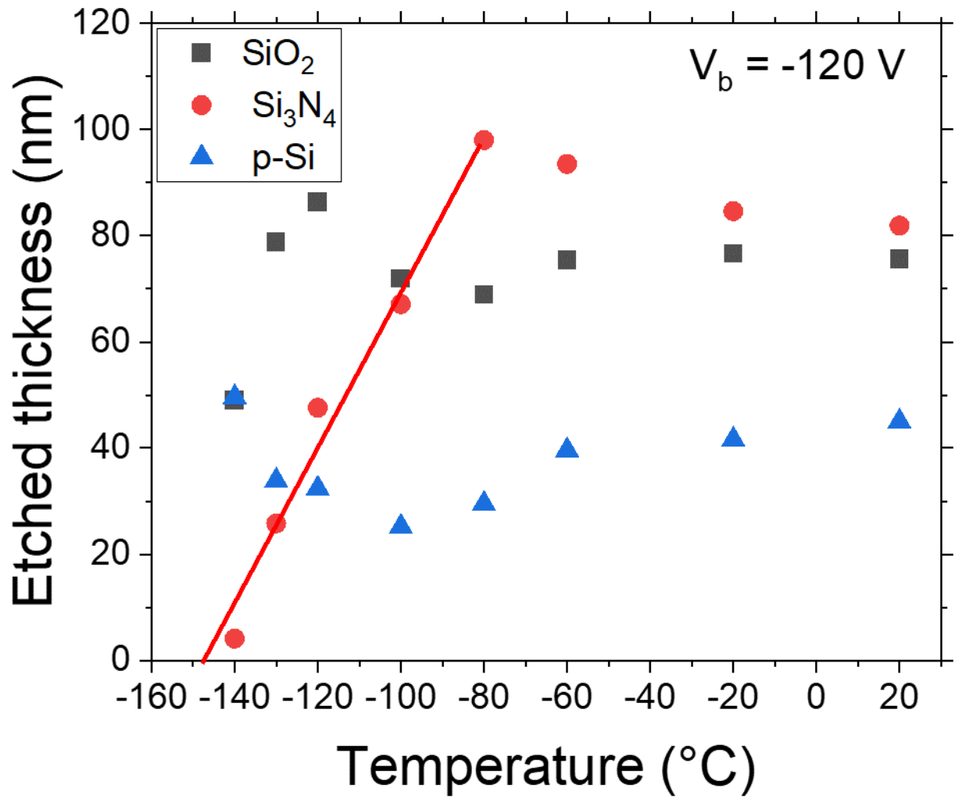

AIP Publishing
Journal of Applied Physics
ACCEPTED MANUSCRIPT

PLEASE CITE THIS ARTICLE AS DOI: 10.1063/5.0142056

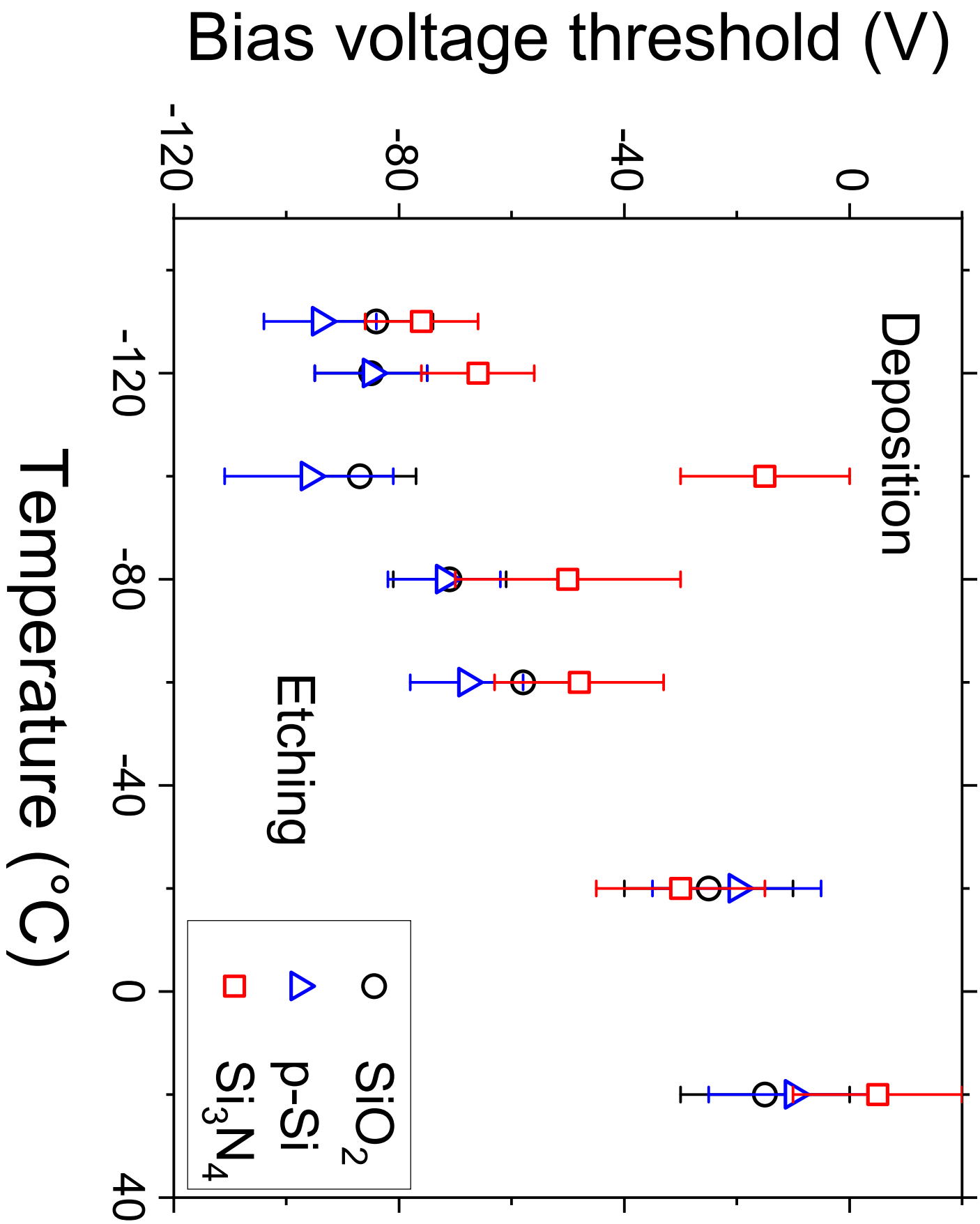

AIP Publishing

Journal of Applied Physics

ACCEPTED MANUSCRIPT

This is the author's peer reviewed, accepted manuscript. However, the online version of record will be different from this version once it has been copyedited and typeset.
PLEASE CITE THIS ARTICLE AS DOI: 10.1063/5.0142056

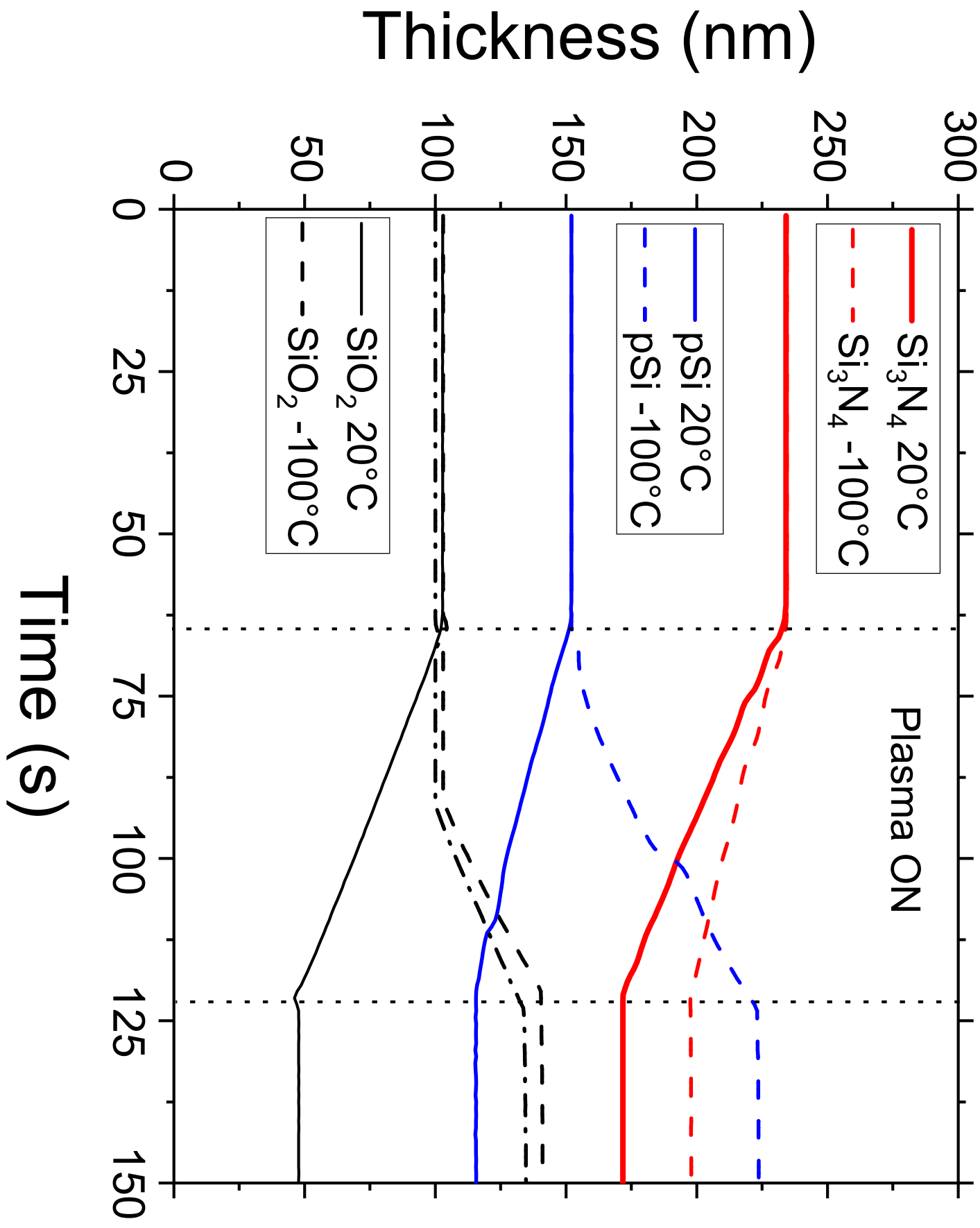

Journal of Applied Physics
AIP Publishing

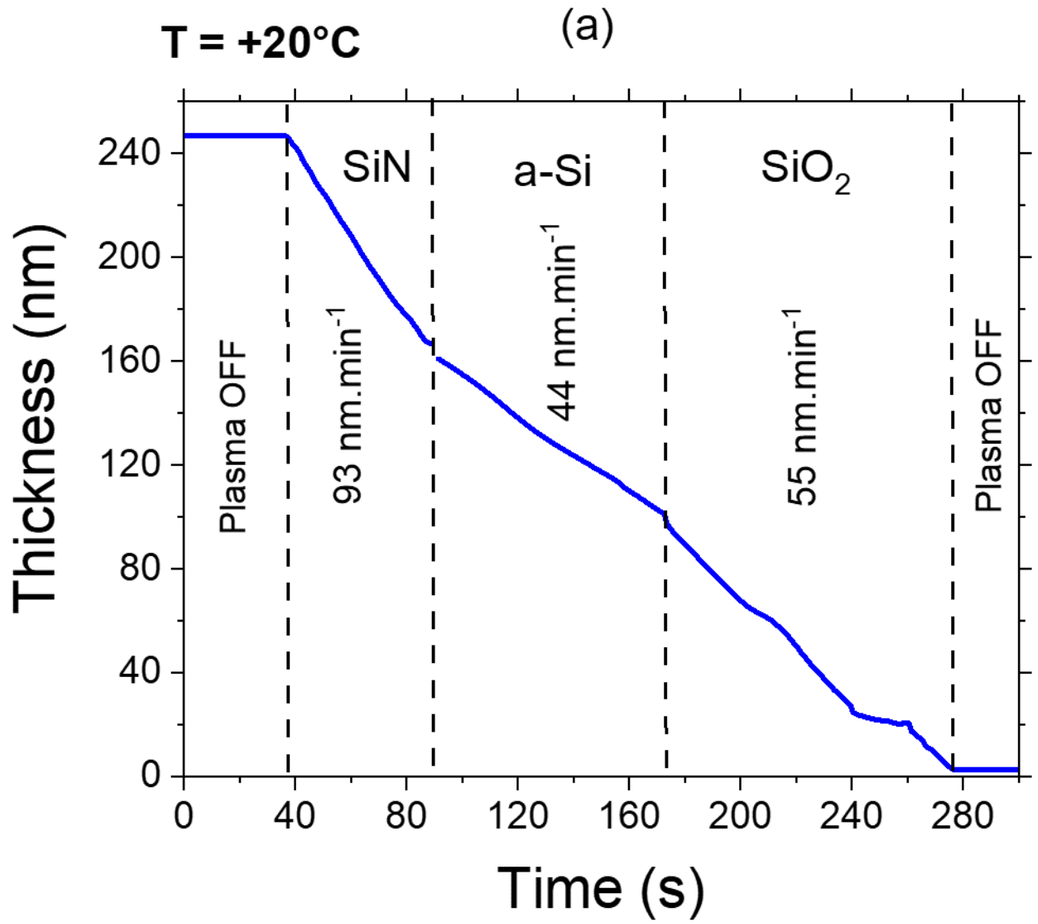

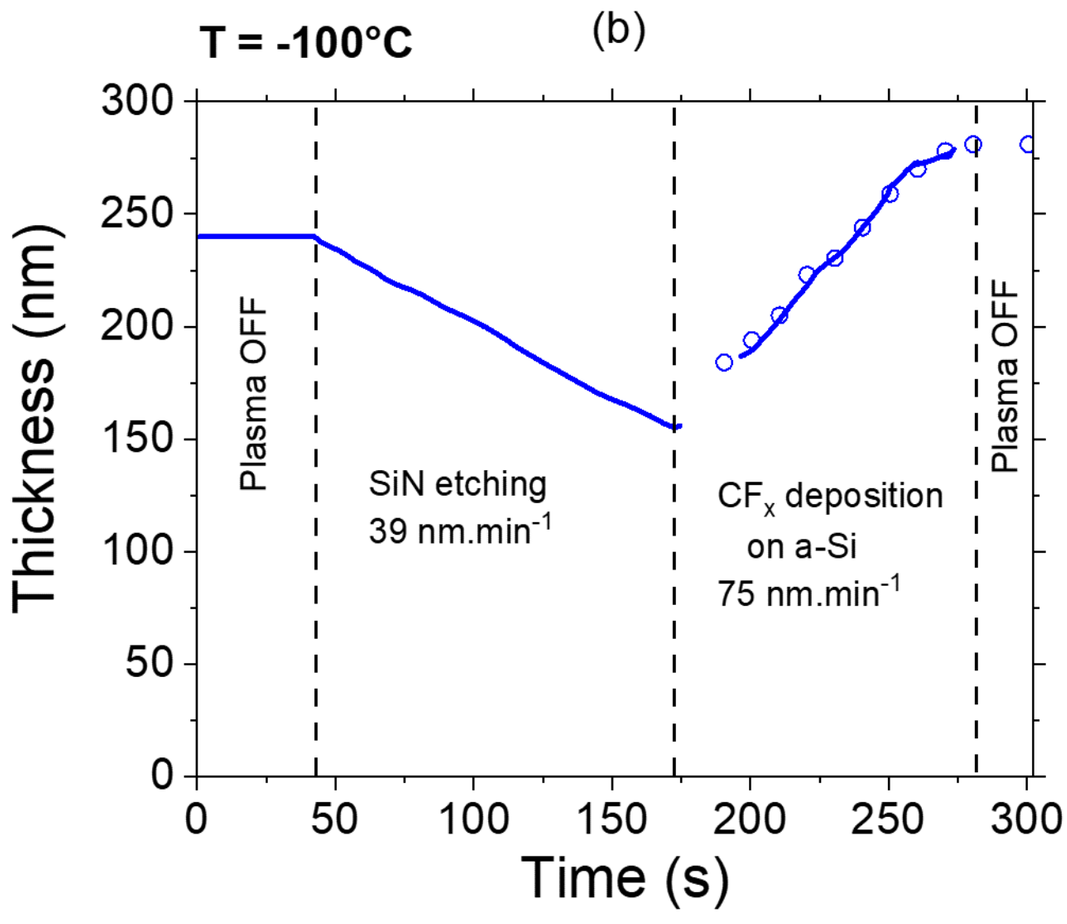

Journal of Applied Physics

AIP Publishing